

Modeling of SiC Lateral Resonant Devices Over a Broad Temperature Range

Russell G. DeAnna*, Shuvo Roy**, Christian A. Zorman**, Mehran Mehregany**

*U.S. Army Research Laboratory, Vehicle Technology Center,
NASA Lewis Research Center, Cleveland, OH 44135

**Microfabrication Laboratory, Department of Electrical Engineering & Computer Science
Case Western Reserve University, Cleveland, OH 44106

ABSTRACT

Finite-element analysis (FEA) modal results of 3C-SiC lateral resonant devices anchored to a Si substrate are presented as resonant frequency versus temperature. The suspended elements are etched from a 2 μm , 3C-SiC film grown at 1600 K on a 500 μm -thick, Si substrate. The analysis includes, temperature-dependent properties, shape change due to volume expansion with temperature, and thermal stress caused by differential thermal expansion of different materials. Two designs are considered: type I has anchor locations close to the geometric centroid and a small shuttle; type II has a large shuttle with anchors far from the centroid. The resonant frequency decreases approximately 3.5% over a 1000 K temperature increase for the type-I device, and behaves according to theory. The resonant frequency of the type-II device decreases by 2% over the first 400 K, then rises slightly over the remaining 600 K. This device deviates from theory because of the high thermal stress induced in the beams. The thermal stress is caused by the differential thermal expansion of the suspended element relative to the substrate. The results show that the device geometry must be properly chosen if the resonant frequency of that device will be used to calculate the temperature coefficient of Young's modulus. These results apply only to resonators of one material on a substrate of a different material.

INTRODUCTION

Micromachined, polysilicon resonators are being studied for mechanical filters, gyroscopes, and accelerometer applications. Lateral resonators are one of the standard devices being used to determine mechanical properties like Young's modulus, residual stress, and structural damping coefficients. SiC is potentially a more attractive material for these devices because of its higher elastic modulus and excellent high-temperature mechanical and electrical properties.

The resonant frequency change with temperature has been used to calculate the temperature coefficient of Young's modulus. One experiment determined the resonant-frequency temperature coefficient for a polysilicon resonator of $-17 \text{ ppm}/^\circ\text{C}$ [1]. Other experiments found $-25 \text{ ppm}/^\circ\text{C}$ for a polysilicon device on a Si substrate and $-10 \text{ ppm}/^\circ\text{C}$ for a SiC device on a Si substrate [2,3].

According to theory, two temperature coefficients influence the resonant frequency of the typical, folded-beam resonator: Young's modulus and thermal expansion. When the device and substrate are of different materials, and the anchors

are not located at a single point, the differential expansion between device and substrate creates thermal stress and the resonant frequency deviates from theory. To gain an understanding of the importance of this thermal stress, two designs are considered: one with anchor locations close together and one where the anchor locations are far apart.

THEORY

The resonant frequency of a folded-beam resonator is governed by [1]

$$f_r^2 = \frac{24EI}{L^3M} \quad (1)$$

E is Young's modulus, I is the beam moment of inertia, L is the beam length, and M is the effective mass of the structure. M is constant with temperature and can be neglected in this discussion. Using the linear coefficient of thermal expansion, α , and the Young's modulus temperature coefficient, α_E , and the resonant frequency temperature coefficient, α_f , equation 1 can be written as

$$(1 + \alpha_f T)^2 \propto (1 + \alpha_E T)(1 + \alpha T) \quad (2)$$

where T is the change of temperature. Expanding terms gives

$$(1 + 2\alpha_f T + \alpha_f^2 T^2) \propto (1 + (\alpha_E + \alpha)T + \alpha_E \alpha T^2) \quad (3)$$

Typical values (for SiC) α and α_E are 4×10^{-6} and -32×10^{-6} , respectively. Hence, the quadratic terms can be neglected with less than a 1% error for temperature differences up to 2000 K. The resonant frequency change with temperature then becomes

$$1 + 2\alpha_f T \propto 1 + (\alpha_E + \alpha)T \quad (4)$$

which can be simplified to

$$2\alpha_f \propto \alpha_E + \alpha \quad (5)$$

The Young's modulus coefficient is negative and several times larger than the thermal expansion coefficient, which explains the experimentally observed decrease in resonant frequency with temperature. Equation 5 does not include any thermal stress induced in the moving element due to differential thermal expansion between device and substrate. It must not

be used to determine either of the temperature coefficients if the resonating device has large thermal stress.

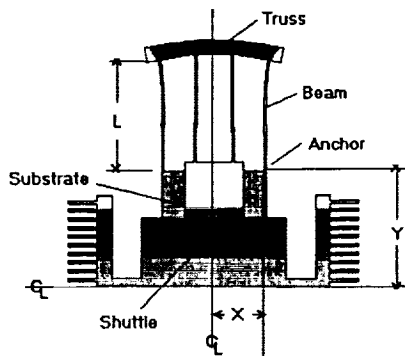


Figure 1: Geometry of the folded-beam structure.

Figure 1 shows the geometry of a typical folded-beam device. When the suspended element expands with temperature more than the substrate, there is a tensile axial stress induced in the beams anchored to the substrate and a compressive stress in the beams attached to the shuttle.

ANALYSIS PROCEDURE

The ANSYS54 [4] finite-element package was used to predict the resonant-frequency as a function of temperature for the two devices shown in Figure 2. The type-I device has anchors close together and a small shuttle; the type-II device has a large shuttle with anchors far apart. Type-I devices should have low thermal stress and closely follow equation 2; type-II devices should have high thermal stress and deviate from equation 2. The beams are $100\text{ }\mu\text{m}$ long by $2\text{ }\mu\text{m}$ wide in the type-I device and $150\text{ }\mu\text{m}$ by $3\text{ }\mu\text{m}$ in the type-II device.

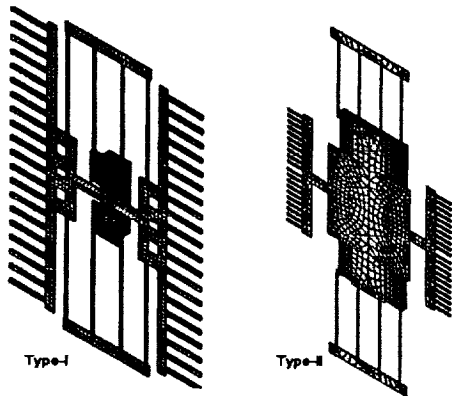


Figure 2: FEM geometries showing type-I and type-II devices.

The finite-element modal (FEM) includes the substrate region between the anchor locations. This allows the anchor locations to move with the thermal expansion of the substrate. Approximately $12\text{ }\mu\text{m}$ of substrate thickness needs to be modeled for accurate results. The thickness can be estimated by comparing the product of Young's modulus and thickness for the device and substrate. For accurate results, the substrate

thickness, Young's-modulus product should be five or more times greater than the product for the device.

Both models have a $1.5\text{ }\mu\text{m}$ -thick layer of silicon dioxide (SiO_2) on the Si substrate. SiC is then grown on the SiO_2 layer in the type-I device. The type II device has an extra $3.5\text{-}\mu\text{m}$ layer of polysilicon between the SiO_2 and SiC. A close up of the substrate and anchor regions is shown in Figure 3 for the type I device and in Figure 4 for the type II device.

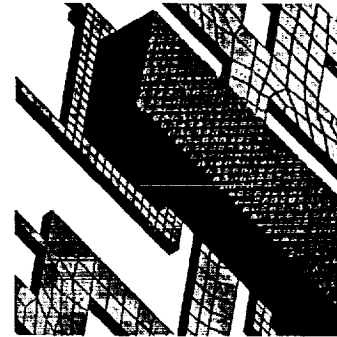


Figure 3: Close-up of anchor and substrate shown up-side-down for type I.

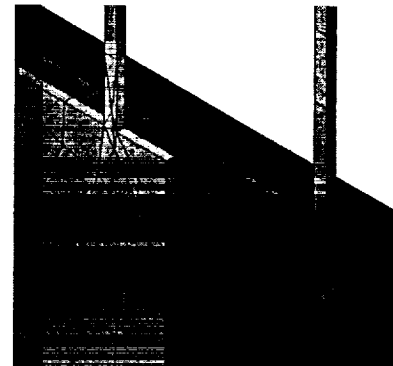


Figure 4: Close up of anchor and substrate for type II.

The bottom of the substrate was fixed in the z-direction (normal to the surface) and allowed free x-y thermal expansion in the plane of the device. Two rows of 8-node bricks were used across the thickness of device. The type-I device was also run with two rows of 20-node bricks. Using 20-node bricks, the lateral mode resonant frequency changes were less than 0.2% for all the temperatures compared to the 8-node-brick results. Type-II results using one row of 8- or 20-node elements across the thickness were different. These results show that three nodes across the thickness are sufficient for accurate results. One, quadratic element containing three nodes should be more accurate than two linear elements with a total of three nodes. Accurate thermal expansion coefficients are necessary for accurate results. Figure 5 shows those values for Si and SiC as a function of temperature [5,6]. Table 1 gives the other properties used in the analysis. According to various experimental studies, values for the Young's modulus temperature coefficient of Si were found between 25 and $80\text{ ppm}/^\circ\text{C}$; SiC values were found between 10 and $46\text{ ppm}/^\circ\text{C}$ [2,3]. The largest values were used in this study.

Table 1 : Material properties used in the finite-element analysis.

Material	Density (kg/m^3)	Young's modulus coefficient ($10^{-6}/K$)	Thermal expansion coefficient ($10^{-6}/K$)	Young's modulus (GPa)
SiC	3230	-46	Figure 5 [5]	250
Si	2320	-80	Figure 5 [6]	160
SiO ₂	2000	-46	0.734	100

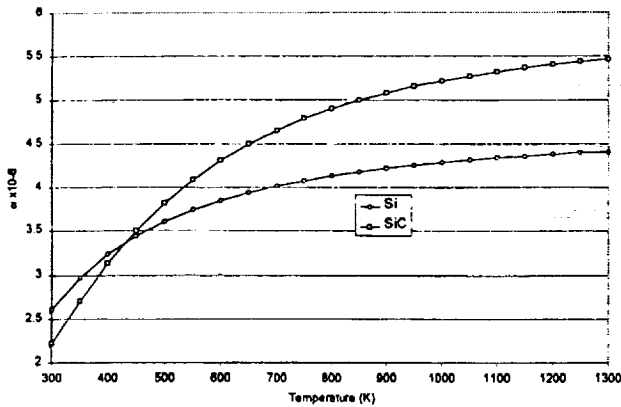


Figure 5: Thermal expansion coefficient of Si and SiC versus temperature [5,6].

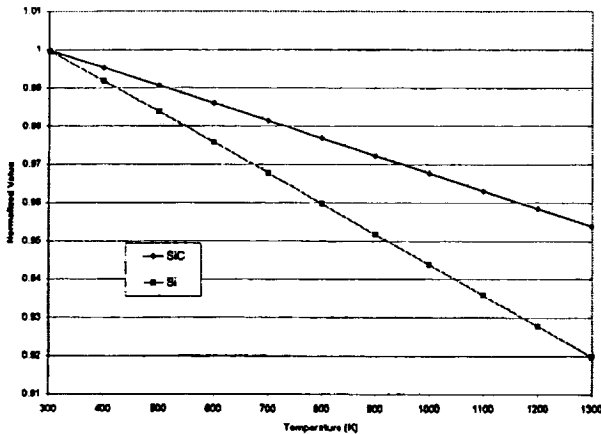


Figure 6: Normalized Young's modulus for SiC and Si versus temperature according to the data of Table 1.

Figure 6 shows the normalized Young's modulus between 300 and 1300 K according to the coefficients given in Table 1.

The analysis was done in two steps: (1) a static analysis to determine the thermal stress and shape change for an applied, uniform temperature; (2) a modal analysis based on the stress and new shape. Results include temperature-dependent properties, thermal stress, and thermal shape change. Results were obtained from 300 to 1300 K in steps of 100 K.

RESULTS

The first four mode shapes for the devices are shown in Figures 7 and 8. In both cases, the lateral mode is the third, the second mode is out of the plane, and modes one and four are rocking or tilting.

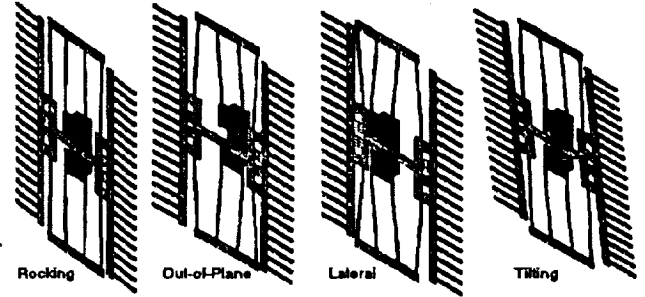


Figure 7: Mode shapes for type-I device.

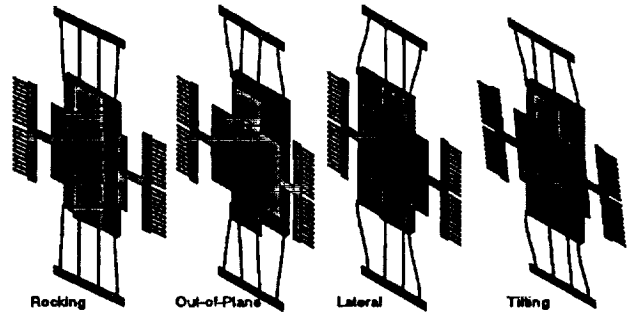


Figure 8: Mode shapes for type-II device.

The room-temperature frequencies for each of the devices and mode shapes are given in Table 2.

Figure 9 shows the lateral mode normalized frequency as a function of temperature for the two devices. Also included in Figure 9 are the experimental data from reference [3] for a device similar to that of type II. The experimental device was also SiC on a Si substrate, with a large shuttle and widely-spaced anchors. Hence, it should behave like the type-II device. According to Figure 6, the normalized Young's modulus over the 1000 K temperature range drops by 4.5%. If the Young's modulus temperature coefficient completely governed the resonant frequency with temperature, the resonant frequency would also decrease by one-half of 4.5% (see equation 5). However, according to equation 5, the resonant frequency also depends on the coefficient of thermal expansion, which is positive. Since the thermal expansion coefficient is positive and nonlinear with temperature, the resonant frequency curve should not decrease as fast as one-half the Young's modulus curve, and should be nonlinear.

As shown in Figure 9, the resonant frequency of the type-I device decreases nonlinearly by 3.5% between 300 and 1300 K. Using the material properties of SiC, this behavior agrees with the theory according to equation 5. It shows that thermal

Table 2: Nominal resonant frequencies for modes one through four.

Device	Resonant Frequency (kHz)			
	Mode I	Mode II	Mode III	Mode IV
Type-I	23	39	43	49
Type-II	7	12	21	25

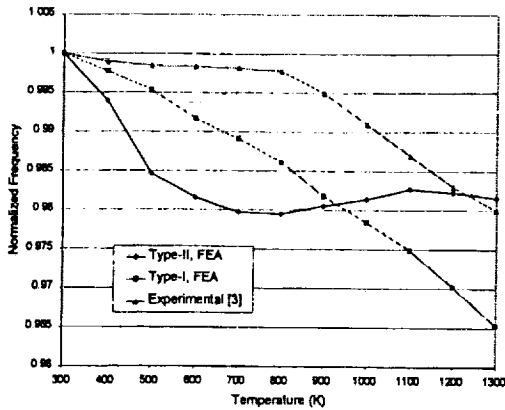


Figure 9: Frequency of the lateral mode versus temperature.

stress is low in the type-I device, and that the substrate material has negligible effect.

As shown in Figure 9, the resonant frequency versus temperature for the type-II device decreases by 2% between 300 and 700 K, then rises slightly with temperature up to 1300 K. This behavior cannot be explained by the theory according to equation 5. The behavior can be explained by considering the thermal-expansion coefficients of both SiC device and the Si substrate. Below 700 K, the Si substrate expands faster than the SiC device. This causes compressive stress in the outer beams. The inner beams are in tension. Most of the stress occurs in the outer beams because the relatively stiff truss partially isolates the inner beams. The beam stress contributes to the frequency decrease caused by the lower Young's modulus. The frequency drops rapidly. The opposite occurs above 700 K. Above 700 K, the SiC device grows faster than the Si substrate and the stress in the beams reverses. This offsets the decrease due to the dropping Young's modulus, and causes the resonant frequency to remain constant. The FEA results frequency curve for the type-II device does not agree with that obtained from the experiment, but the overall frequency change does agree. The knee in each case occurs around 700 K, which corresponds to the point where the thermal expansion of SiC equals that of Si. This difference is under investigation.

CONCLUSIONS

In a two-material lateral-resonating device, anchor spacing and shuttle size may influence the resonance frequency with temperature. A device with closely-spaced anchors, should behave according to theory, and should not be influenced by the thermal expansion of the substrate. This type

of device would be suitable for experiments to determine the temperature coefficient of Young's modulus. The resonant frequency versus temperature curve, in this case, corresponds to equation 5. The results show that if the device has widely-spaced anchors, the substrate thermal expansion influences the resonant frequency. High thermal stress develops in the beams, which causes an unusual curve of frequency versus temperature. For accurate finite-element modeling, it is important to include the substrate material between the anchors to allow differential thermal expansion between device and substrate.

If the primary purpose of a lateral-resonating device is the experimental determination of the temperature coefficient of Young's modulus, a geometry like the type-I device (small shuttle and anchors close together) is proper. A device like type II with large shuttle and widely-space anchors should not be used to calculate the Young's modulus temperature coefficient. These conclusions only apply to lateral-resonating devices where the material of the suspended or moving element differs from that of the substrate.

REFERENCES

- [1] M. Biebl, G. Brandl, and R. T. Howe, "Young's Modulus of in Situ Phosphorus-Doped Polysilicon," The 8th International Conference on Solid-State Sensors and Actuators, and Eurosensors IX, Stockholm, Sweden, June 25-29, 1995.
- [2] A. J. Fleischman, S. Roy, C. A. Zorman, and M. Mehregany, "Behavior of Polycrystalline SiC and Si Surface-Micromachined Lateral Resonant Structures at Elevated Temperatures," Proc. of the IEEE Intl. Conf. On Silicon Carbide, III-Nitrides, and Related Matls., ICSCIII-N 97, pp. 889-892, 1998.
- [3] A. J. Fleischman, X. Wei, C. A. Zorman, and M. Mehregany, "Surface Micromachining of Polycrystalline SiC Deposited on SiO_2 by APCVD," Proc. of the IEEE Intl. Conf. On Silicon Carbide, III-Nitrides, and Related Matls., ICSCIII-N 97, pp. 885-888, 1998.
- [4] ANSYS, Inc., Canonsburg, PA 15317.
- [5] R.R. Reeber and K. Wang, "Thermal expansion and lattice parameters of group IV semiconductors," Mat. Chem. And Phys 46, 259-264, 1996.
- [6] R.R. Reeber and K. Wang in Thermal Expansion of β -SiC, GaP and InP, Mater. Res. Soc. Symp. Proc. 410, pp. 211-216, 1996.